

1 Postprint, accepted in Journal of Biogeography

2

3 **Original article**

4

5 **Running header:** Karstificability and dispersal in a subterranean species

6

7 **Substratum karstificability, dispersal and genetic structure in a strictly**
8 **subterranean beetle**

9

10

11 Valeria Rizzo¹, David Sánchez-Fernández^{1,2}, Rocío Alonso¹, Josep Pastor³ and Ignacio
12 Ribera^{1*}

13

14 ¹*Institute of Evolutionary Biology (CSIC-Universitat Pompeu Fabra), Barcelona, Spain*

15 ²*Instituto de Ciencias Ambientales. Universidad de Castilla-La Mancha. Campus*

16 *Tecnológico de la Fábrica de Armas, Toledo, Spain*

17 ³*Museu de Ciències Naturals (Zoologia), Barcelona, Spain*

18

19 *Correspondence: I. Ribera, Institute of Evolutionary Biology, Passeig Maritim de la
20 Barceloneta, 37-49, 08003, Barcelona, Spain.

21 E-mail: ignacio.ribera@ibe.upf-csic.es

22

23 **Word count (from Abstract to References): 7361**

24 1 small, 2 medium and 1 large (tree) figures

25 1 small, 1 medium table

26

27

28 **ABSTRACT**

29 **Aim** The deep subterranean environment is an ideal system to test the effect of physical
30 constraints on the ecology and evolution of species, as it is very homogeneous and with
31 simple communities. We studied the effect of substratum karstificability in the dispersal
32 of the strictly subterranean *Troglocharinus ferreri* (Reitter) (Coleoptera, Leiodidae) by
33 comparing the genetic diversity and structure of populations in limestone (more soluble)
34 and dolostone (less soluble) in the same karstic system.

35 **Location** *Troglocharinus ferreri* is only known from ca.100 vertical shafts in an area of
36 less than 500 km² SW of Barcelona (Spain).

37 **Methods** We sequenced mitochondrial and nuclear markers of a representative sample
38 to identify main lineages within *T. ferreri* and estimate their temporal origin, and used
39 mitochondrial data of 129 specimens from 41 caves to reconstruct their demographic
40 history and estimate dispersal among caves.

41 **Results** *Troglocharinus ferreri* diverged from its sister in the Early Pliocene, with an
42 initial divergence of the sampled populations in the Early Pleistocene. The best
43 demographic model was a constant population size with a fast population increase in the
44 middle Pleistocene. The ancestral population was likely in limestone, with a probability
45 of transition from limestone to dolostone triple to that from dolostone to limestone,
46 suggesting a higher permeability of limestone to the transit of individuals. Populations
47 in dolostone caves had lower gene flow between them and a stronger isolation by
48 distance, although the low genetic variability for the studied markers and the lower
49 abundance of dolostone caves decreased the statistical power of the analyses.

50 **Main conclusions** Our results point to the physical characteristic of the substratum as a
51 determinant of dispersal and gene flow, potentially conditioning the long-term evolution
52 of subterranean biodiversity.

53

54 **Keywords**

55 Gene flow, isolation, substratum permeability, subterranean environment,

56 *Troglocharinus*, troglomorphism

57

58 INTRODUCTION

59 It has long been recognised that some physical properties of the habitats may constraint
60 the characteristics of the organisms living in them. Some of these constraints may affect
61 dispersal and gene flow between populations, thus potentially also acting at longer,
62 evolutionary time scales. This general principle has been articulated in different
63 theoretical frameworks (see e.g. Grime, 1977 for plants, or the "habitat templet" of
64 Southwood, 1977 for terrestrial invertebrates), but it has been difficult to precisely
65 identify which habitat characteristics determine these constraints, especially those
66 promoting dispersal, divergence and speciation. Some of the best studied examples
67 include long-term habitat stability, especially in aquatic systems, both marine (mediated
68 through the type of larval development, e.g. Emler, 1995) and freshwater (Ribera &
69 Vogler, 2000; see Ribera, 2008 for a review). In terrestrial systems, likely due to their
70 higher complexity, it has been more difficult to identify habitat characteristics linking
71 processes affecting individuals or populations to those affecting metapopulations or
72 species, and ultimately whole lineages (but see Papadopoulou *et al.*, 2009 for an
73 example with Coleoptera).

74 A system that potentially may simplify this complexity is the deep subterranean
75 environment. In the deep parts of caves and the associated network of voids and fissures
76 the environmental conditions of the habitat are extremely constant and homogeneous,
77 with a permanent darkness and nearly constant humidity and temperature through the
78 year, which is approximately equal to the average annual temperature of the surface
79 (Racovitza, 1907; Poulson & White, 1969; Culver & Pipan, 2009). Subterranean
80 organisms have a very limited range of options to take advantage of local climatic
81 heterogeneities, and their general lack of mobility reduces the possibility of migration
82 when conditions become unfavourable. In addition, the general scarcity of resources in
83 the deep subterranean environment imposes stringent requirements on the species,
84 resulting in simple communities showing low local diversity (Poulson & Culver, 1969;
85 Culver, 1976).

86 The subterranean environment is a discontinuous medium with a highly variable
87 degree of connectivity, and populations of troglobitic species are in general more
88 fragmented than populations of species living on the surface (Crouau-Roy, 1989; Culver
89 & Pipan, 2009). Due to the difficulty to disperse, gene flow among geographically close
90 populations can be very restricted, resulting in a strong micro-endemism (Juberthie *et*
91 *al.*, 1980; Faille *et al.*, 2015a,b). These conditions offer a particularly favourable

92 situation for exploring the relationship between environmental factors and the genetic
93 structure of populations, as due to the geographical proximity and the generally
94 homogeneous environment the number of confounding variables should be greatly
95 reduced.

96 One of the main factors potentially constraining dispersal within the
97 subterranean environment is the karstificability of the substratum, which is highly
98 dependent on its lithology and geochemical composition. The role of geological barriers
99 (i.e. non karstifiable strata) has been traditionally recognised as a factor shaping the
100 distribution and evolution of the subterranean fauna (e.g. Bellés, 1973; Bellés &
101 Martínez, 1980), and the degree of fragmentation of the karst has recently being related
102 with ongoing speciation processes in some Pyrenean subterranean species (Faille *et al.*,
103 2015a,b). These studies, however, did not establish a direct link between the geology of
104 the substratum and the genetic structure of the studied species, and the factors
105 potentially affecting dispersal could not be identified with precision. Ideally, the role of
106 karstificability in determining dispersal and genetic structure should be investigated
107 with populations of the same species in different geological substrata, but otherwise
108 with similar general characteristics and with the same biogeographic history.

109 Here we study a system that matches these conditions, the troglobitic species
110 *Troglocharinus ferreri* (Reitter) (Coleoptera, Leioididae, Leptodirini) in the
111 subterranean environment of the Garraf massif, in the vicinity of Barcelona (NE of the
112 Iberian peninsula). In a previous study we found that this strictly subterranean genus
113 expanded its range from the central Pyrenees to the coastal area of Catalonia in the early
114 Pliocene, where it subsequently diversified during the late Pliocene and the Pleistocene
115 (Rizzo *et al.*, 2013). Within the coastal clade of the genus *Troglocharinus*, *T. ferreri* is
116 distributed in the Garraf massif, isolated by Pleistocene sedimentary basins of three
117 rivers (Llobregat in the north-east, Anoia in the north and Foix in the southwest, Fig. 1).
118 Preliminary results suggested a high level of genetic diversity within *T. ferreri*,
119 consistent with the complex geological structure of the plateau of the Garraf massif
120 (Rizzo *et al.*, 2013), with one mitochondrial lineage mostly associated with a more
121 homogenous limestone of Cretaceous origin and its sister (including a recognised
122 subspecies, *T. ferreri pallaresi* Bellés) inhabiting also some areas with Jurassic and
123 Triassic dolostone. Dolomite ($\text{CaMg}(\text{CO}_3)_2$) has a similar structure to calcite but with
124 approximately half of its Ca replaced by Mg. The dissolution rate of dolomite is
125 considerably lower than that of calcite (Goldscheider & Drew, 2007), and in a recent

126 study Appelo & Postma (2005) estimated that under the same chemical and physical
127 conditions of the water it takes more than 100 times longer to reach 95% saturation for
128 dolomite than for calcite. In addition, erosion in dolomitic karsts results in fine sand that
129 fills sinkholes and caves, partially blocking the ground water circulation and further
130 reducing the development of a subterranean medium (Renault, 1970; Gilli, 2015). This
131 lower karstificability should result in an environment less permeable for the
132 subterranean fauna, with impeded dispersal and reduced contact between populations in
133 different areas of the massif.

134 Using a comprehensive sample of *T. ferreri* across the different geologic layers
135 found through its entire geographic range we investigate the relationship between the
136 karstificability of the substratum and the genetic diversity and structure of the
137 populations living on it, which may be an indication of differences in the rate of
138 dispersal between them. Since we compare individuals in a reduced geographical space,
139 originating from the same colonization event and with a shared evolutionary history and
140 the same ecology, biology and physiology, it is expected that differences among them
141 are mainly the result of the geology of the substratum in which they are found. Our
142 specific objectives are (1) determine the phylogeographic structure and demographic
143 history of *T. ferreri* within its entire distributional range; (2) reconstruct the direction
144 and frequency of the transitions between different types of substratum; and (3) compare
145 the genetic structure of populations within geological layers with different degrees of
146 karstificability.

147

148 **MATERIALS AND METHODS**

149 **Geological and taxonomic background**

150 The Garraf Massif is a calcareous horst with an area of around 500 km² in the north-east
151 of the Iberian Peninsula, 30 km south-west of the city of Barcelona. It is part of the
152 Catalanian littoral cordillera, composed mainly of Jurassic and Cretaceous limestone
153 and dolostone and isolated by Quaternary sedimentary layers from the rest of the coastal
154 area (Daura *et al.*, 2014; Figs 1,2). The central part of the massif is dominated by
155 Cretaceous limestone rocks (Moreno, 2007), where most of the karst formations have
156 developed, while the Jurassic dolomite strata in the high plains present less significant
157 karst development and fewer dolines (Rubinat, 2004). Outcrops of Cretaceous marls and
158 marly limestone are also found in a few areas (Moreno, 2007), while the Triassic
159 carbonates comprise strata that only crop out in the north-east of the Garraf Massif rim

160 (Fig. 2). There are more than three hundred shafts documented in the central Garraf
161 Massif, which have been explored since the late 19th century (Cardona i Oliván, 1990),
162 in which the fauna is well documented due to the long biospeleological tradition of the
163 city of Barcelona (e.g. Zariquieyi, 1917; Lagar, 1954; Español, 1961; Bellés, 1973).

164 *Troglocharius ferreri* currently includes three recognised subspecies, *T. ferreri*
165 *ferreri*, *T. ferreri pallaresi* and *T. ferreri abadi* Lagar, all restricted to the Garraf Massif
166 (Salgado *et al.*, 2008; Fresneda & Salgado, 2017). Four other subspecies were described
167 based mostly on small differences in the shape of the pronotum and the antennae, but
168 are now considered to be synonyms of *T. ferreri ferreri* due to the presence of multiple
169 populations with intermediate morphologies (Salgado *et al.*, 2008; Appendix S1a). The
170 two recognised subspecies were maintained in part due to the geologic isolation of their
171 populations (Salgado *et al.*, 2008). *Troglocharinus ferreri ferreri* is known from 123
172 cavities distributed through the Garraf Massif (Fresneda & Salgado, 2017; Appendix
173 S2a), although this number may certainly increase with additional explorations. The
174 other two subspecies have, however, very restricted distributions: *T. ferreri abadi* is
175 only known from three cavities in close proximity situated in the northwest of the
176 Massif, and *T. ferreri pallaresi* from four cavities in the north-east, also in close
177 proximity (Fresneda & Salgado, 2017).

178

179 **Taxon sampling and DNA sequencing**

180 We sequenced a total of 126 specimens of *T. ferreri ferreri* from 40 shafts distributed
181 through its entire known distribution area, and three *T. ferreri pallaresi* from the type
182 locality (Avenc de Montmany) (Fig. 2; Appendix S1a). Caves were chosen with the aim
183 to include the whole range of geographic, geologic and taxonomic diversity, including
184 the type locality of the species (Avenc d'en Roca) and those of the synonymised
185 subspecies, of which we obtained two (Appendix S1a). Despite several attempts we
186 could not obtain specimens of *T. ferreri abadi* for study, and we are not aware of recent
187 records (the last collected specimens to our knowledge being from Cova Miserachs in
188 1987, J. Comas personal communication, 2015). The three shafts in which the
189 subspecies is known are very dry, and the specimens, always in reduced numbers, have
190 only being found in the deepest, more humid areas (Salgado *et al.*, 2008).

191 Specimens were collected in caves with the use of baits laid 24h in advance or
192 through manual searches. We sequenced five specimens of each cave whenever
193 available (Appendix S1a). Virtually all cavities in the Garraf Massif are vertical shafts

194 with no or very limited horizontal development, and in most cases beetles were
195 collected at the base of the shaft, so the coordinates of the entrance are a good
196 approximation to the actual location of the samples. To increase the statistical power of
197 some analyses of molecular diversity we pooled specimens from caves known to be part
198 of the same system, connected through the subterranean medium and without any
199 apparent geological discontinuity between them (Fig. 2; Appendix S1a).

200 DNA extractions of single specimens were non-destructive, using commercial
201 kits (mostly DNeasy Tissue Kit, Qiagen, Hilden, Germany) following the
202 manufacturer's instructions. Vouchers and DNA samples are kept in Institute of
203 Evolutionary Biology, Barcelona (IBE). We amplified fragments of five mitochondrial
204 and four nuclear genes in eight amplification reactions: (1) 5' end (the "barcode", *coxI*-
205 5') and (2) 3' end of the cytochrome c oxidase subunit (*coxI*-3'); (3) an internal fragment
206 of the cytochrome oxidase b (*cob*); (4) 5' end of the large ribosomal unit plus the
207 Leucine transfer plus the 3' end of NADH dehydrogenase subunit 1 (*rrnL+trnL+nad1*);
208 (5) 5' end of the small ribosomal unit, 18S rRNA (*SSU*); (6) an internal fragment of the
209 large ribosomal unit, 28S rRNA (*LSU*); and one fragment each of (7) the histone H3
210 (*H3*) and (8) wingless (*Wg*) (see Appendix S2b for the primers used, and Appendix S1a
211 for the specimens sequenced for each of the fragments). Owing to the generally low
212 levels of variability found in preliminary analyses, only a limited sample of specimens
213 was sequenced for the nuclear markers (Appendix S1a). New sequences (285) were
214 deposited in the EMBL database under accession numbers LT797170- LT797446,
215 LT799421- LT799428) (Appendix S1a).

216

217 **Phylogenetic and phylogeographic analyses**

218 We aligned the gene fragments with MAFFT 6 ([http://mafft.cbrc.jp/alignment/](http://mafft.cbrc.jp/alignment/server) server).
219 Protein-coding genes were aligned using the FFT-NS-1 algorithm, and ribosomal genes
220 with the Q-INS-i algorithm, which considers the secondary structure (Kato *et al.*,
221 2009).

222 To reconstruct the general phylogenetic relationships and time of divergence
223 among the main lineages within *T. ferreri* we built a data matrix with all mitochondrial
224 and nuclear markers, using as outgroups a selection of 26 specimens from both the
225 coastal and Pyrenean clades of *Troglocharinus* following the topology obtained in
226 Rizzo *et al.* (2013) (Appendix S1a). We reconstructed phylogenetic relationships with
227 RAxML 7 (Stamatakis *et al.*, 2008) using GTR+I+G as an evolutionary model and a

228 partition by gene, separating the two *cox1* fragments (due to the unequal sampling) and
229 pooling the two mitochondrial ribosomal genes (*rrnL+trnL*). The optimum topology
230 was that of the best likelihood amongst 100 replicates, and node support was estimated
231 with 500 bootstrap replicates using the CAT approximation (Stamatakis *et al.*, 2008).
232 We analysed the nuclear sequence data separately using the same methods.

233 To obtain an estimation of the divergence time we analysed the matrix in
234 BEAST 1.8 (Drummond *et al.*, 2012), using as priors the rates obtained by Cieslak *et al.*
235 (2014) for the same group of organisms and genes, calibrated using the tectonic
236 separation of Sardinia from mainland Europe ca. 33 Ma (Schettino & Turco, 2006). We
237 used an uncorrelated relaxed clock with normally distributed prior average rates of
238 0.015 substitutions/site/MY for mitochondrial protein coding genes (*cox1-5*, *cox1-3*,
239 *cob*, *nad1*), 0.004 for nuclear ribosomal (*LSU*, *SSU*), and 0.006 for mitochondrial
240 ribosomal genes (*rrnL+trnL*), all of them with a standard deviation of 0.001. For the
241 nuclear protein coding genes (*H3*, *Wg*) we used default flat priors. We constrained the
242 monophyly of the coastal and Pyrenean clades respectively, following the topology
243 obtained in Rizzo *et al.* (2013) and ran two independent analyses for 200 million (M)
244 generations, logged every 5000, with 20 M (10%) as burn-in fractions. Preliminary
245 analyses with the complete matrix using either a Yule speciation (YL) or a Birth-Death
246 with incomplete sampling model (BD, Stadler, 2009) failed to converge, so we used a
247 sample of 27 specimens of *T. ferreri* with complete sequence data, including all main
248 lineages as identified in the RAXML analysis and a wide representation of different
249 caves and types of substratum. We used a GTR+I+G and HYK evolutionary models for
250 each of the two mitochondrial and nuclear partitions respectively, and TRACER 1.6
251 (Drummond *et al.*, 2012) to assess convergence, measure the effective sample size of
252 each parameter and check that the used burn-in fraction was sufficient. We run two
253 different sets of analyses using YL or BD models, comparing their likelihoods using
254 100 replicas of the Akaike's Information Criterion for MCMC samples (AICM) statistic
255 (known to perform better than harmonic mean estimators, Baele *et al.*, 2013) in
256 TRACER 1.6.

257

258 **Demographic history**

259 To estimate the demographic history of *T. ferreri* we used the mitochondrial *cox1-5*
260 fragment only, for which the sampling was most complete and presented sufficient
261 variation, with a GTR+I+G evolutionary model and an a-priori mean rate of 0.015

262 substitutions/site/MY with a standard deviation of 0.001. We run two analyses in
263 BEAST 1.8, one with a strict clock and a second with a relaxed lognormal, and
264 comparing their likelihoods using 100 replicas of the AICM statistic. Analyses were run
265 for 100 M generations and convergence and burn-in fraction were assessed as in
266 previous BEAST analyses.

267 We compared four demographic models implemented in BEAST 1.8: constant
268 population size (CT), population expansion (ES), logistic growth (LG) and exponential
269 growth (EL). We also constructed a Bayesian skyline plot (BSP, Drummond *et al.*,
270 2005) with the results of a separate analysis. The likelihood of the trees built with the
271 different models were compared with 100 replicas of the AICM statistic.

272

273 **Estimation of transition rates between different geological substrata**

274 To estimate the transition rates between different geological substrates we assigned each
275 of the caves to different categories according to the dissolvability of the substratum in
276 which they are found, as estimated with detailed lithological maps (ICC, 2010;
277 Appendix S1a). We divided the caves in two categories: (1) Cretaceous limestone and
278 (2) Jurassic and Triassic dolostone. Due to the lower number of dolostone caves we
279 pooled all dolostone caves in a single category. We did an ancestral trait reconstruction
280 in BEAST 1.8, with the geological type of the cave as a discrete character and a reduced
281 *cox1-5* matrix randomly selecting one specimen per cave when multiple haplotypes in
282 the same cave were monophyletic (Appendix S1a). We used a single partition with a
283 simple HKY model with estimated nucleotide frequencies, as preliminary analyses
284 showed convergence problems when using more complex models. We set up an
285 asymmetric discrete phylogeographic (CTMC) model (Lemey *et al.*, 2009), using as
286 priors a uniform distribution between 0 and 1 for the frequencies, and a Gamma with
287 shape 1 and scale 1 for the rates. We also implemented the best clock and demographic
288 model as estimated above and uniform root frequencies for the trait. The analyses were
289 run for 100 M generations, and convergence was assessed as in the previous analyses.

290

291 **Genetic versus geologic or geographic distances**

292 To estimate the role of the lithology in the genetic isolation among *T. ferreri*
293 populations we compared the relationship between phylogenetic and geographical
294 distances in populations in dolostone and limestone. Given the heterogeneity of the
295 spatial distribution of dolostone and limestone in the Garraf massif, in addition to the

296 simple geographic distance between caves we also used a weighted measure taking into
297 account the permeability to the subterranean fauna of the different geological substrata
298 in between them.

299 Phylogenetic distances were obtained in MESQUITE 3.8
300 (<http://mesquiteproject.org>) from the ultrametric tree obtained with the *cox1-5* sequence,
301 using the best demographic and clock models as estimated previously. Geographic
302 distances were measured from the cave entrance and specimens from the same cave
303 were considered to have a geographic distance of zero. These distances were expressed
304 in decimal degrees and calculated in ARCGIS 9.3 (ESRI, Redlands, CA, USA). For the
305 geological data we used the “Mapa de grups litològics de Catalunya LITO250M_v1
306 (2010)” downloaded from the Institut Cartogràfic i Geològic de Catalunya
307 (www.igc.cat), converted into a raster file at a resolution of 0.001° (c. 90 m). We pooled
308 all dolostone caves (Jurassic and Triassic) in a single category, and added two non-
309 karstifiable layers (with no known caves), recognising a total of four layers: (1)
310 Cretaceous limestone; (2) Jurassic and Triassic dolostone; (3) sedimentary rocks with
311 no or few carbonated constituents (mainly marly limestone); (4) metamorphic or
312 sedimentary siliceous rocks (marls, slate) (Fig. 2; Appendixes S1a,S2c). We assigned a
313 value of geological resistance to each one of these categories as a proxy of the
314 suitability for the dispersal of the subterranean fauna, with lower values for cells with
315 higher geologic permeability (i.e. low resistance). We tested the sensitivity of our
316 results to different values of resistance by trying five different combinations, always
317 maintaining the ranking of substratum resistance (1<2<3<4) (Appendix S2c).

318 We used the software CIRCUITSCAPE 2.2 (McRae, 2006; McRae *et al.*, 2008)
319 to estimate the pairwise connectivity (or current flow) between the cells with observed
320 presences (i.e. caves with fauna) according to the five resistance maps (Appendixes
321 S2c,d). CIRCUITSCAPE uses circuit theory to model connectivity in heterogeneous
322 landscapes. Landscapes are represented as conductive surfaces, with low resistances
323 assigned to landscape features types that are most permeable to movement or best
324 promote gene flow, and high resistances assigned to movement barriers. We selected
325 the pairwise option so that connectivity, or current flow, was calculated between all
326 pairs of observed presence cells, and these pairwise current maps were then overlapped
327 (and averaged) to obtain a single cumulative current (or connectivity) map (Appendix
328 S2d).

329 The values of these five cumulative connectivity maps were then correlated
330 (Pearson's correlation coefficient) with genetic distances using a Mantel test with 1000
331 randomizations, to estimate whether the phylogenetic distance between populations in
332 caves in different substratum was best explained by geographic distance alone or by a
333 compound measure of geologic isolation and geographic distance.

334

335 **Genetic diversity and population structure**

336 We compared population genetic statistics between caves from different geological
337 substrata, to test if their different karstificability resulted in significant differences in
338 dispersal among populations that could be reflected in their current genetic
339 characteristics. Caves were classified as being on limestone or dolostone as described
340 above (Appendix S1a). To increase the number of specimens per population, when
341 caves were in the same substratum, in close proximity and within the same geological
342 unit (i.e. without any geological or lithological discontinuity) we pooled individuals
343 within the same clade following the topology of the previous phylogeographic analyses
344 (Appendix S1a). We collapsed the *cox1-5* haplotypes of each population in Mesquite v3
345 and estimated *Fst* values between caves in ARLEQUIN v3.5 (Excoffier *et al.*, 2005).
346 We then compared the slope of the regression between geographic distance and *Fst*. If
347 due to the lower permeability of the substratum nearby caves in dolostone are more
348 isolated between them than caves in limestone, the *Fst* value should increase at a higher
349 rate with geographic distance, resulting in a steeper slope. For each cave we identified
350 all caves within a radius of 5 km using ARCGIS 9.3 and plotted the geographical
351 distance (km) against the *Fst*. We separated three types of caves pairs considering the
352 type of substratum, limestone-limestone, limestone-dolostone and dolostone-dolostone,
353 and estimated the slope of the linear regression for each of them.

354

355 **RESULTS**

356 **Phylogenetic and phylogeographic analyses**

357 The complete final data set (Appendix S1a) included 5173 aligned nucleotides, with no
358 length variation except for some regions in the *LSU* gene and a variation of one or two
359 Asparagine residues in a repetitive region in the gene *Wg*. The topology of the coastal
360 clade of *Troglocharinus* was very similar to that obtained in Rizzo *et al.* (2013), with *T.*
361 *ferreri* monophyletic and sister to the rest of the species with very good support. Within
362 *T. ferreri* two well-supported clades were recovered (clades 1 and 2), although with

363 only moderate support for most of the internal nodes in each of them (Appendix S3a).
364 The nuclear sequence only recovered a monophyletic *T. ferreri*, although with low
365 support, and with no support for internal relationships (Appendix S3b).

366 In the calibrated analysis in BEAST with a representative sample of *T. ferreri*
367 the best tree model was BD (AICM YL= 28674.8, BD= 28625.4), although with a
368 poorer convergence. The topology and age estimations of both analyses were, however,
369 almost identical, with changes in some poorly supported terminal nodes (Appendix
370 S3c,d). The separation between the coastal and Pyrenean clades was estimated to have
371 occurred at the end of the Miocene-early Pliocene (5 +/- 1 Ma), with the separation
372 between *T. ferreri* and the rest of species in close proximity (4.5 +/-1 Ma). The sampled
373 *T. ferreri* had a last common ancestor in the transition Pliocene-Pleistocene (2.6 +/- 0.6
374 Ma), and most of the variation within the different lineages of *T. ferreri* had a Middle to
375 Late Pleistocene origin (Appendix S3c).

376

377 **Demographic history**

378 The analysis of the *cox1-5* data (129 specimens, Appendix S1a) assuming a strict clock
379 had better AICM than when assuming a lognormal clock (AICM strict= 4072.6;
380 relaxed= 4084.2). In all subsequent analyses using the *cox1-5* data we thus implemented
381 a strict clock.

382 The best demographic model was constant population size (CT) (Table 1). The
383 Bayesian skyline plot (Fig. 3) suggested no substantial changes for most of the history
384 of the species, with a rapid population growth starting at ca. 250-300 Kya and a
385 pronounced shift at <100 Kya. In all subsequent analyses we implemented a CT model.

386 The Bayesian tree obtained with a strict clock and a CT coalescent model had
387 good support for the two main clades within *T. ferreri* (Fig. 4), but only moderate or
388 poor support for most of the lineages. Most haplotypes found in single caves were either
389 exclusive or only found in other caves in close geographical proximity. Only one cave
390 had individuals with mitochondrial haplotypes in the two main clades, the Avenç San
391 Cristofol, and only three had individuals with haplotypes in different well supported
392 lineages within each of the clades (Cuneta, Sogre and Bufi) (Figs 2,4). All four caves
393 with individuals of mixed origins were in limestone (Appendix S1a). Of the 13 caves in
394 dolostone, none had individuals with haplotypes in different main lineages, although
395 due to the higher number of limestone caves (28) differences were not significant as
396 measured with a Fisher's exact test in a 2x2 contingency table.

397

398 **Estimation of transition rates between geological substrata**

399 The reduced matrix selecting one specimen per cave when all sampled specimens were
400 monophyletic had 82 haplotypes (Appendix S1a). The most likely lithology of the
401 ancestral population was reconstructed as limestone, with a probability of 0.74 over
402 0.24 dolostone (Fig. 4). Similar probabilities were reconstructed for clade 2 (0.6 versus
403 0.4), while clade 1 was clearly reconstructed as having originated from limestone caves
404 (0.98, Fig. 4). Within clade 1 there were some transitions to Jurassic or Triassic
405 dolostones, but all very recent and with only one potential reversal to limestone. This
406 reversal affected two caves (Roca and Rigol) at ca. 1.3 km from each other but in
407 different geological substratum (limestone and Jurassic dolostone respectively), which
408 populations had specimens with mixed haplotypes (Fig. 4). Within clade 2 there was
409 one genetically and geologically isolated lineage sister to the rest, *T. ferreri pallaresi* in
410 Montmany cave, in Triassic dolostones (Fig. 4). The remaining specimens were
411 grouped in two poorly supported clades, one entirely on limestone caves (clade 2A) and
412 the other reconstructed as having originated in Jurassic dolostone with only 56%
413 probability (clade 2B). Within the later there was only one reversal to limestone,
414 affecting two caves (Cristofol and Bufi) also in close proximity (ca. 0.6 Km) and
415 surrounded by dolostone. In both caves there were also specimens with haplotypes
416 belonging to other clades in limestone caves (Fig. 4), suggesting that they have a fauna
417 of mixed origin.

418 There were large differences in the geographic setting of the different clades.
419 Clade 1 (limestone, with only some caves in Jurassic dolostone) occupies a large
420 geographic area within the Garraf massif (mean geographic distance between caves of
421 7.0 km); while the two lineages within clade 2 (2A in limestone and 2B in Jurassic
422 dolostone) both occupy a restricted area with a mean geographic distance between caves
423 in each of them of 1.2 km (Fig. 2).

424 The estimated transition rate from limestone to dolostone was ca. three times
425 that of dolostone to limestone (1.46 vs. 0.51), although with largely overlapping
426 marginal probability distributions (Fig. 4).

427

428 **Genetic versus geologic or geographic distances**

429 The correlation between geographic and phylogenetic distance was strongly significant
430 both for the whole *T. ferreri* and for the two clades separately, with or without the

431 inclusion of *T. ferreri pallaresi* (Montmany cave) (Table 2). None of the schemes with
432 different values for the geological resistance could improve the correlation obtained
433 with the simple geographical distance (Table 2), although the best (also with highly
434 significant correlations) was the one with the highest resistance values for sedimentary
435 and metamorphic rocks, which do not have void interstices (Table 2, Appendix S2c).
436 The phylogenetic distances within the two main clades were very similar but, as noted
437 above, clade 1 covers a much wider area (Fig. 2), which resulted in significantly
438 different slopes of the regression lines between genetic and geographic distances (Table
439 2). Thus, in clade 2, with both dolostone and limestone caves, the same phylogenetic
440 distances were attained at much shorter distances than in clade 1, mostly with limestone
441 caves.

442

443 **Genetic structure in populations in limestone vs dolostone**

444 The relationship between geographical distance and *Fst* for caves closer than 5 km was
445 non significant for pairs of caves in limestone (N= 188, $y = 0.38+0.04x$; $p = 0.37$; $r^2 =$
446 0.02). This relationship was significant for pairs of caves in different substratum
447 (limestone-dolostone; N= 146, $y = 0.39+0.07x$; $p = <0.01$; $r^2 = 0.06$), and especially for
448 pairs of caves in dolostone, with a higher slope (N= 22, $y = 0.28+0.14x$; $p < 0.001$; $r^2 =$
449 0.50).

450

451 **DISCUSSION**

452 Despite the reduced extension of its geographic range, *T. ferreri* displays a strong
453 phylogeographic structure, as could be expected from a strictly subterranean species
454 with very limited dispersal capabilities (Kane *et al.*, 1992). This phylogeographic
455 variation, together with the general homogeneity of the subterranean environment and
456 the lack of climatic differences due to its limited geographic range, render subterranean
457 species ideal systems to study the effect of physical constraints imposed by the habitat
458 (see e.g. Faille *et al.*, 2015a,b for examples with a different group of Coleoptera).

459 According to our reconstruction, and in agreement with Rizzo *et al.* (2013), the
460 ancestor of the coastal clade of the genus *Troglocharinus* colonized the area at the end
461 of the Pliocene-early Pleistocene, likely in a window of favourable climatic conditions
462 before the onset of the Mediterranean climate ca. 3.2 Ma (Suc, 1984). This range
463 expansion from the ancestral area in the Pyrenees to the coast may have involved
464 surface displacements, as there is no continuity in the subterranean medium between the

465 Pyrenean and coastal areas (Rizzo *et al.*, 2013). The resistance of the species of
466 *Troglocharinus* to relatively high temperatures (up to 20-23°C, Rizzo *et al.*, 2015)
467 would allow surface displacements in periods with low seasonality and high
468 precipitation, such as the Pliocene-Pleistocene transition (Suc & Cravatte, 1982;
469 Jiménez-Moreno *et al.*, 2010). The subsequent formation of sedimentary basins in the
470 rivers surrounding the Garraf massif likely contributed to the isolation of the
471 populations that would become the current *T. ferreri* (Rizzo *et al.*, 2013).

472 The demographic reconstruction suggested a constant population size for most
473 of the history of the species but with a fast population expansion starting at ca. 0.3 Ma.
474 This expansion is in agreement with the available data of the development of the
475 subterranean environment in the Garraf massif (Daura *et al.*, 2014). According to these
476 authors, the caves in the Garraf plateau have an endogenous origin, and the subterranean
477 network of cavities and fissures did not developed completely, opening to the surface,
478 before the middle-upper Pleistocene. The accessibility to an extensive subterranean
479 system in the massif could have allowed the population expansion of *T. ferreri*. It must
480 be noted that the ancestor of the coastal clade of *Troglocharinus* (and thus of *T. ferreri*)
481 must have had all the morphological and physiological modifications currently
482 associated with the subterranean life (Rizzo *et al.*, 2013; Cieslak *et al.*, 2014), so it
483 could be expected that the subterranean environment was occupied whenever it become
484 accessible.

485 We found a highly significant linear correlation between geographic and
486 phylogenetic distance in all main lineages within *T. ferreri*, despite the reduced
487 geographic area. This correlation is habitually interpreted as isolation by distance
488 (Slatkin, 1993), without dispersal barriers or corridors that could respectively increase
489 or decrease isolation with independence of geographic distance. Within the Garraf
490 Massif the subterranean environment is not continuous, as there are geological
491 discontinuities and non-calcareous layers which in principle should act as barriers to
492 dispersal through the underground. This was apparent in the case of the subspecies *T.*
493 *ferreri pallaresi*, isolated from the rest of the populations by a layer of non karstifiable
494 Triassic Keuper marl (ICC, 2010). However, and contrary to our expectations, the
495 attempt to weight geographic distances with a-priori values for the permeability to
496 dispersal of the different substrata did not result in any improvement in the correlation
497 with phylogenetic distance, although the best result was obtained with the highest
498 resistance values for non-karstifiable materials (sedimentary and metamorphic rocks).

499 It must be considered that, although highly significant, this correlation was relatively
500 small, with low slopes and a high dispersion except when the geographically and
501 genetically very isolated population of *T. ferreri pallaresi* was included in the analyses.
502 The low variance explained by distance alone suggests a more complex scenario, with
503 possibly a number of uncontrolled factors determining dispersal acting at small scales,
504 although it may just be that our exploration of the parametric space was insufficient.

505 Other than the possible existence of what could be considered strong barriers,
506 preventing all movement through the subterranean habitat, the different composition of
507 the substratum did also influence the dispersal capabilities and in consequence the
508 genetic structure of the studied populations. The Garraf Massif is broadly divided in two
509 bands of different composition perpendicular to the coast, limestone in the south and
510 dolostone in the north (Fig. 2). Our results suggest that the initial colonization was in
511 limestone, more soluble and thus likely to have developed a subterranean network of
512 fissures earlier than the dolostone. The initial colonization of limestone may have biased
513 the estimation of the transition probabilities (Davis *et al.*, 2013), which had also wide
514 marginal distributions likely due to the low number of dolostone caves. But in any case,
515 our results indicate a much higher rate of transitions from limestone to dolostone than
516 vice-versa, suggesting that limestone is more permeable to the movements of the
517 subterranean fauna. This higher permeability agrees with the fact that in most dolostone
518 caves only closely related specimens were found, in many cases forming a
519 monophyletic lineage exclusive of a cave or a group of caves in close geographic
520 proximity, although differences with limestone caves were not statistically significant. It
521 is interesting to note that the limestone caves with fauna of mixed origin were all in the
522 same area, and in close proximity of the caves in dolostone inhabited by populations of
523 clade 2 (see the location of the caves in Fig. 2). There is the possibility that other factors
524 favoured the transit of the subterranean fauna in this area, including some early
525 transitions from limestone to dolostone in this clade. The high number of tectonic faults
526 (ICC, 2010) may be one of these factors.

527 The general relationship between phylogenetic and geographic distances was
528 also indicative of differences between the permeability of dolostone and limestone to
529 the movement of the subterranean fauna. Thus, the clade with the highest proportion of
530 dolostone caves (clade 2) had a steeper slope than the clade mostly on limestone caves
531 (clade 1), suggesting a lower permeability to the displacement of the fauna. A similar
532 result was obtained for the degree of genetic isolation (as measured with the *F_{st}*)

533 between the population of a cave and that of its closest neighbours. For caves in
534 dolostone *Fst* values increased much faster with distance than when caves were in
535 limestone, clearly indicating a stronger isolation likely due to the increased difficulty of
536 displacement through the substratum.

537 There are few systems in which it is possible to trace the effect of a physical
538 constraint from the individual to the macroevolution of the lineage. In this sense, the
539 highly fragmented subterranean habitat offers an excellent opportunity, with the
540 additional advantage of its abiotic and biotic simplicity and stability. Knowing the
541 factors leading to the origin of the current diversity can greatly help to inform
542 management and conservation decisions, but the lack of data of both genetic diversity
543 and population viability in this unique system hampers our understanding of the
544 potential effect of environmental changes (Rizzo *et al.*, 2015; Sánchez-Fernández *et al.*,
545 2016).

546

547 **ACKNOWLEDGEMENTS**

548 We thank Aliga speleo Group of Barcelona, Jordi Comas, Javier Fresneda and Enric
549 Lleopart for help and support in the field; Pau Balart, Ana Izquierdo and Arnaud Faille
550 for laboratory work, and Jordi Comas for multiple comments and suggestions on the
551 distribution and taxonomy of *T. ferreri*. We also thank the editor (Isabel Sanmartín) and
552 three referees for the useful comments to earlier versions of the manuscript. DS-F was
553 supported by a “Juan de la Cierva” postdoctoral contract from the Spanish Ministry of
554 Economy and Competitiveness and another post-doctoral contract funded by
555 Universidad de Castilla-La Mancha and the European Social Fund (ESF). This work
556 was partly funded by projects CGL2010-15755 and CGL2016-76705-P (AEI/FEDER,
557 UE) to IR.

558

559 **REFERENCES**

- 560 Appelo, C.A.J. & Postma, D. (2005) *Geochemistry, groundwater and pollution*. CRC
561 press, Boca Raton, Florida.
- 562 Baele, G., Li, W.L.S., Drummond, A.J., Suchard, M.A. & Lemey, P. (2013) Accurate
563 model selection of relaxed molecular clocks in Bayesian phylogenetics.
564 *Molecular Biology and Evolution*, **30**, 239–243.
- 565 Bellés, X. (1973) Un nuevo Bathysciinae del Macizo de Garraf. *Miscelánea Zoológica*,
566 **3**, 45–49.

- 567 Bellés, X. & Martínez, A. (1980) La geología y la especiación de los Bathysciinae en la
568 región del Penedès (Catalunya, España). *Mémoires de Biospéologie*, **7**, 221–223.
- 569 Cardona i Oliván, F. (1990) *Grans cavitats de Catalunya, segon volum: El sistema*
570 *mediterrani i la Depressió Central*. Espeleo Club de Gracia, Barcelona.
- 571 Cieslak, A., Fresneda, J. & Ribera, I. (2014) Life-history specialization was not an
572 evolutionary dead-end in Pyrenean cave beetles. *Proceedings of the Royal*
573 *Society B, Biological Sciences*, **281**, 20132978.
- 574 Crouau-Roy, B. (1989) Population studies on an endemic troglobitic beetle:
575 geographical patterns of genetic variation, gene flow and genetic structure
576 compared with morphometric data. *Genetics*, **121**, 571–582.
- 577 Culver, D.C. (1976) The evolution of aquatic cave communities. *American Naturalist*,
578 **110**, 945–957.
- 579 Culver, D.C. & Pipan, T. (2009) *The biology of caves and other subterranean habitats*.
580 Oxford University Press, Oxford.
- 581 Daura, J., Sanz, M., Forno, J.J., Asensio, A. & Juliá, R. (2014) Karst evolution of the
582 Garraf Massif (Barcelona, Spain): doline formation, chronology and archaeo-
583 palaeontological archives. *Journal of Cave and Karst Studies*, **76**, 69–87.
- 584 Davis, M.P., Midford, P.E. & Maddison, W. (2013) Exploring power and parameter
585 estimation of the BiSSE method for analyzing species diversification. *BMC*
586 *Evolutionary Biology*, **13**, 38.
- 587 Drummond, A.J., Rambaut, A., Shapiro, B. & Pybus, O.G. (2005) Bayesian coalescent
588 inference of past population dynamics from molecular sequences. *Molecular*
589 *Biology and Evolution*, **22**, 1185–1192.
- 590 Drummond, A.J., Suchard, M.A., Xie, D. & Rambaut, A. (2012) Bayesian
591 Phylogenetics with BEAUti and the BEAST 1.7. *Molecular Biology and*
592 *Evolution*, **29**, 1969–1973.
- 593 Emler, R.B. (1995) Developmental mode and species geographic range in regular sea
594 urchins (Echinodermata: Echinoidea). *Evolution*, **49**, 476–489.
- 595 Español, F. (1961) Fauna cavernícola de la provincia de Barcelona 1: Invertebrados.
596 *Catálogo Espelológico de la Provincia de Barcelona*, **1**, 29–46.
- 597 Excoffier, L., Smouse, P.E. & Quattro, J.M. (1992) Analysis of molecular variance
598 inferred from metric distances among DNA haplotypes: application to human
599 mitochondrial DNA restriction data. *Genetics*, **131**, 479–491.

600 Excoffier, L., Laval, G. & Schneider, S. (2005) Arlequin (version 3.0): an integrated
601 software package for population genetics data analysis. *Evolutionary*
602 *Bioinformatics online*, **1**, 47.

603 Faille, A., Bourdeau, C., Bellés, X. & Fresneda, J. (2015a) Allopatric speciation
604 illustrated: The hypogean genus *Geotrechus* Jeannel, 1919 (Coleoptera:
605 Carabidae: Trechini), with description of four new species. *Arthropod*
606 *Systematics and Phylogeny*, **73**, 439–455.

607 Faille A., Tänzler, R. & Toussaint, E.F.A. (2015b) On the way to speciation: Shedding
608 light on the karstic phylogeography of the micro-endemic cave beetle
609 *Aphaenops cerberus* in the Pyrenees. *Journal of Heredity*, **106**, 692–699.

610 Fresneda, J. & Salgado, J.M. (2017) Catálogo de los Coleópteros Leiodidae Cholevinae
611 Kirby, 1837 de la península Ibérica e islas Baleares. *Monografies del Museu de*
612 *Ciències Naturals*, **7**, 1–308.

613 Gilli, E. (2015) *Karstology. Karsts, caves and springs*. CRC Press, Boca Raton, Florida.

614 Goldscheider, N. & Drew, D. (Eds) (2007) *Methods in Karst Hydrogeology: IAH:*
615 *International Contributions to Hydrogeology*. CRC Press, Boca Raton, Florida.

616 Grime, J.P. (1977) Evidence for the existence of three primary strategies in plants and
617 its relevance to ecological and evolutionary theory. *American Naturalist*, **111**,
618 1169–1194.

619 ICC [Institut Cartogràfic de Catalunya] (2010) *Mapa de grups litològics de Catalunya*
620 *1:250.000 LITO250M_v1*. Institut Cartogràfic i Geològic de Catalunya,
621 Barcelona.

622 Jiménez-Moreno, G., Fauquette, S. & Suc, J-P. (2010) Miocene to Pliocene vegetation
623 reconstruction and climate estimates in the Iberian Peninsula from pollen data.
624 *Review of Palaeobotany and Palynology*, **162**, 403–415.

625 Juberthie, C., Delay, B. & Bouillon, M. (1980) Sur l'existence d'un milieu souterrain
626 superficiel en zone non calcaire. *Comptes-rendus de l'Académie des Sciences de*
627 *Paris*, **290(D)**, 49–52.

628 Kane, T.C., Culver, D.C. & Jones, R.T. (1992) Genetic structure of morphologically
629 differentiated populations of the amphipod *Gammarus minus*. *Evolution*, **46**,
630 272–278.

631 Katoh, K., Asimenos, G. & Toh, H. (2009) Multiple alignment of DNA sequences with
632 MAFFT. *Methods in Molecular Biology*, **537**, 39–64.

633 Lagar, A. (1954) Los Bathysciinae de la provincia de Barcelona. *Speleon*, **5**, 247–259.

- 634 Lemey, P., Rambaut, A., Drummond, A.J. & Suchard, M.A. (2009) Bayesian
635 phylogeography finds its roots. *PLoS Computational Biology*, **5**(9), e1000520.
- 636 McRae, B.H. (2006) Isolation by resistance. *Evolution*, **60**, 1551–1561.
- 637 McRae, B.H., Dickson, B.G., Keitt, T.H. & Shah, V.B. (2008) Using circuit theory to
638 model connectivity in ecology and conservation. *Ecology*, **10**, 2712–2724.
- 639 Moreno JA (2007) Bioestratigrafía del Aptiense del macizo del Garraf (NE de la
640 Península Ibérica) *Geogaceta*, **41**, 131–134.
- 641 Papadopoulou, A., Anastasiou, I., Keskin, B., & Vogler, A.P. (2009) Comparative
642 phylogeography of tenebrionid beetles in the Aegean archipelago: the effect of
643 dispersal ability and habitat preference. *Molecular Ecology*, **18**, 2503–2517.
- 644 Poulson, T.L., White, W.B. (1969) The cave environment. *Science*, **165**, 971–981.
- 645 Poulson, T.L. & Culver, D.C. (1969) Diversity in terrestrial cave communities. *Ecology*,
646 **50**, 153–158.
- 647 Racovitza, E.G. (1907) Essai sur les problèmes biospéologiques. *Archives de Zoologie*
648 *Expérimentale et Générale. 4ème série*, **VI**, 371–488.
- 649 Renault, P.H. (1970) *La formation des cavernes, Que Sais-je?* PUF, Paris.
- 650 Ribera, I. (2008) Chapter 15: Habitat constraints and the generation of diversity in
651 freshwater macroinvertebrates. In: *Aquatic Insects: Challenges to Populations*.
652 (eds Lancaster J, Briers RA), pp. 289–311. CAB International, Wallingford, UK.
- 653 Ribera, I. & Vogler, A.P. (2000) Habitat type as a determinant of species range sizes:
654 the example of lotic–lentic differences in aquatic Coleoptera. *Biological Journal*
655 *of the Linnean Society*, **71**, 33–52.
- 656 Rizzo, V., Comas, J., Fadrique, F., Fresneda, J. & Ribera I. (2013) Early Pliocene range
657 expansion of a clade of subterranean Pyrenean beetles. *Journal of Biogeography*,
658 **40**, 1861–1873.
- 659 Rizzo, V., Sánchez-Fernández, D., Fresneda, J., Cieslak, A. & Ribera I. (2015) Lack of
660 evolutionary adjustment to ambient temperature in highly specialized cave
661 beetles. *BMC Evolutionary Biology*, **15**, 10.
- 662 Rubinat, F. (2004) *Catàleg Espeleològic del Massís de l'Ordal: Barcelona*. Centre
663 Excursionista Àliga, Barcelona.
- 664 Sánchez-Fernández, D., Rizzo, V., Cieslak, A., Faille, A., Fresneda, J., & Ribera, I.
665 (2016). Thermal niche estimators and the capability of poor dispersal species to
666 cope with climate change. *Scientific reports*, **6**, 23381.

- 667 Salgado, J.M., Blas, M. & Fresneda, J. (2008) *Fauna Ibérica. Vol. 31: Coleoptera:*
668 *Cholevidae*. CSIC, Madrid.
- 669 Schettino, A. & Turco, E. (2006) Plate kinematics of the Western Mediterranean region
670 during the Oligocene and Early Miocene. *Geophysical Journal International*,
671 **166**, 1398–1423.
- 672 Slatkin, M. (1993) Isolation by distance in equilibrium and non-equilibrium
673 populations. *Evolution*, **47**, 264–279.
- 674 Southwood, T.R.E. (1977) Habitat, the templet for ecological strategies? *Journal of*
675 *Animal Ecology*, **46**, 337–365.
- 676 Stadler, T. (2009) On incomplete sampling under birth-death models and connections to
677 the sampling-based coalescent. *Journal of Theoretical Biology*, **261**, 58–66.
- 678 Stamatakis, A., Hoover, P., & Rougemont, J. (2008) A rapid bootstrap algorithm for the
679 RAxML web servers. *Systematic biology*, **57**, 758–771.
- 680 Suc, J.P. & Cravatte, J. (1982) Étude palynologique du Pliocène de Catalogne (nord-est
681 de l'Espagne). *Paleobiologie Continentale*, **13**, 1–31.
- 682 Suc, J.P. (1984) Origin and evolution of the Mediterranean vegetation and climate in
683 Europe. *Nature*, **307**, 429–432.
- 684 Zariquieyi, R. (1917) Sobre el gènere *Troglocharinus* (Ins. Col.). *Treballs de la*
685 *Institució Catalana d'Història Natural*, **3**, 283–294.
- 686
- 687
- 688

689 **SUPPORTING INFORMATION**

690 Additional Supporting Information may be found in the online version of this article:

691

692 **Appendix S1** Additional materials:

693 (a) List of the studied material.

694

695 **Appendix S2** Additional methods:

696 (a) Location of caves in the Garraf.

697 (b) Primers used in the study.

698 (c) Categorisation of geological substrata and resistance.

699 (d) Resistance maps.

700

701 **Appendix S3** Additional results:

702 (a) Best tree with mitochondrial and nuclear markers.

703 (b) Best tree with only nuclear markers.

704 (c) Tree obtained with a Yule speciation.

705 (d) Tree obtained with a birth death with incomplete sampling.

706

707 **BIOSKETCH**

708 **Valeria Rizzo** is a PhD student in the Institute of Evolutionary Biology in Barcelona.

709 This paper is part of his thesis dissertation, focussed on the evolution of a lineage of
710 subterranean beetles (genus *Troglocharinus*).

711

712 Editor: Isabel Sanmartin

713

714 Author Contributions: V.R. and I.R. conceived the work; V.R., J.P. and I.R. led the
715 specimen and data collection; V.R. and R.A. obtained the molecular data; V.R., D.S-F.
716 and I.R. analysed the data; V.R. and I.R. led the writing and all authors contributed to
717 the discussion of results and writing.

718

719

720

721 **TABLES**

722

723 **Table 1** Value of Akaike's information criterion for MCMC samples (AICM) of the
 724 four tested demographic models. CT, constant population size; ES, population
 725 expansion; LG, logistic growth; EL, exponential growth. Lower values of AICM
 726 indicate a better adjustment to the model.

727

model	AICM	stdv.	Δ AICM
CT	4008.9	0.08	-
ES	4013.3	0.14	-4.4
LG	4046.7	0.21	-37.8
EL	4012.6	0.10	-3.7

728

729

730 **Table 2** Linear regression between phylogenetic distances, Euclidean geographic
 731 distances (in decimal degrees) and distances weighted by resistance schemes A, B & E
 732 (values for C&D were intermediate between B&E, data not shown). See Appendixes
 733 S2c,d for the resistance values applied to the different geologic substrata; and Appendix
 734 S1a and Fig. 4 for the composition of the clades (clade "2(A+B)" refers to Clade 2 with
 735 the exclusion of *T. ferreri pallaresi*).

736

distance	clade	intercept	SE (i)	slope	SE (s)	r2	p
geographic	1	0.22	0.004	1.78	0.051	0.27	<0.01
	2	0.20	0.003	3.57	0.059	0.77	<0.01
	2(A+B)	0.18	0.004	4.91	0.233	0.32	<0.01
A	1	0.32	0.003	0.001	0.001	0.00	n.s.
	2	0.17	0.005	0.02	0.001	0.58	n.s.
	2(A+B)	0.29	0.005	0.01	0.001	0.11	n.s.
B	1	0.29	0.004	0.02	0.002	0.02	n.s.
	2	0.14	0.005	0.08	0.002	0.60	n.s.
	2(A+B)	0.20	0.005	0.04	0.003	0.16	n.s.
E	1	0.21	0.006	0.11	0.005	0.11	<0.01
	2	0.07	0.006	0.24	0.005	0.65	<0.01
	2(A+B)	0.15	0.006	0.13	0.007	0.27	<0.01

737

738

739

740 **FIGURE LEGENDS**

741

742 **Figure 1** Distribution of the coastal clade of the genus *Troglocharinus*, with the main
743 tectonic and geological substrata (modified from Rizzo *et al.*, 2013). Black squares, *T.*
744 *ferreri*; circles, other species in the coastal clade. Colour codes: yellow, Tertiary and
745 Quaternary sedimentary basins; green, folded Mesozoic cover; pink and purple:
746 Hercynian substratum; grey: Quaternary filling of Miocene and Quaternary fractures.
747 Lines represent tectonic features in standard geological notation. Note the isolation of
748 the distribution area of *T. ferreri* by Quaternary sediments.

749

750 **Figure 2** Simplified geological map with the location of the studied caves (circles).
751 Blue, caves in clade 1; yellow, caves in clade 2A (limestone lineage); red, caves in
752 clade 2B (dolostone lineage); black, *T. ferreri pallaresi* (upper right corner). Caves with
753 mixed colours had specimens of different clades. Geological substratum: yellow,
754 dolostone; green, limestone; grey and pink, different non-karstifiable materials
755 (modified from ICC, 2010).

756

757 **Figure 3** Bayesian skyline plot of the analyses of the *coxI-5* matrix of 129 specimens of
758 *T. ferreri*, assuming a strict clock with a rate of 0.015 substitutions/site/MY. Thin lines,
759 95% confidence intervals; horizontal axis, time (MY); vertical axis, effective population
760 size (N_eT).

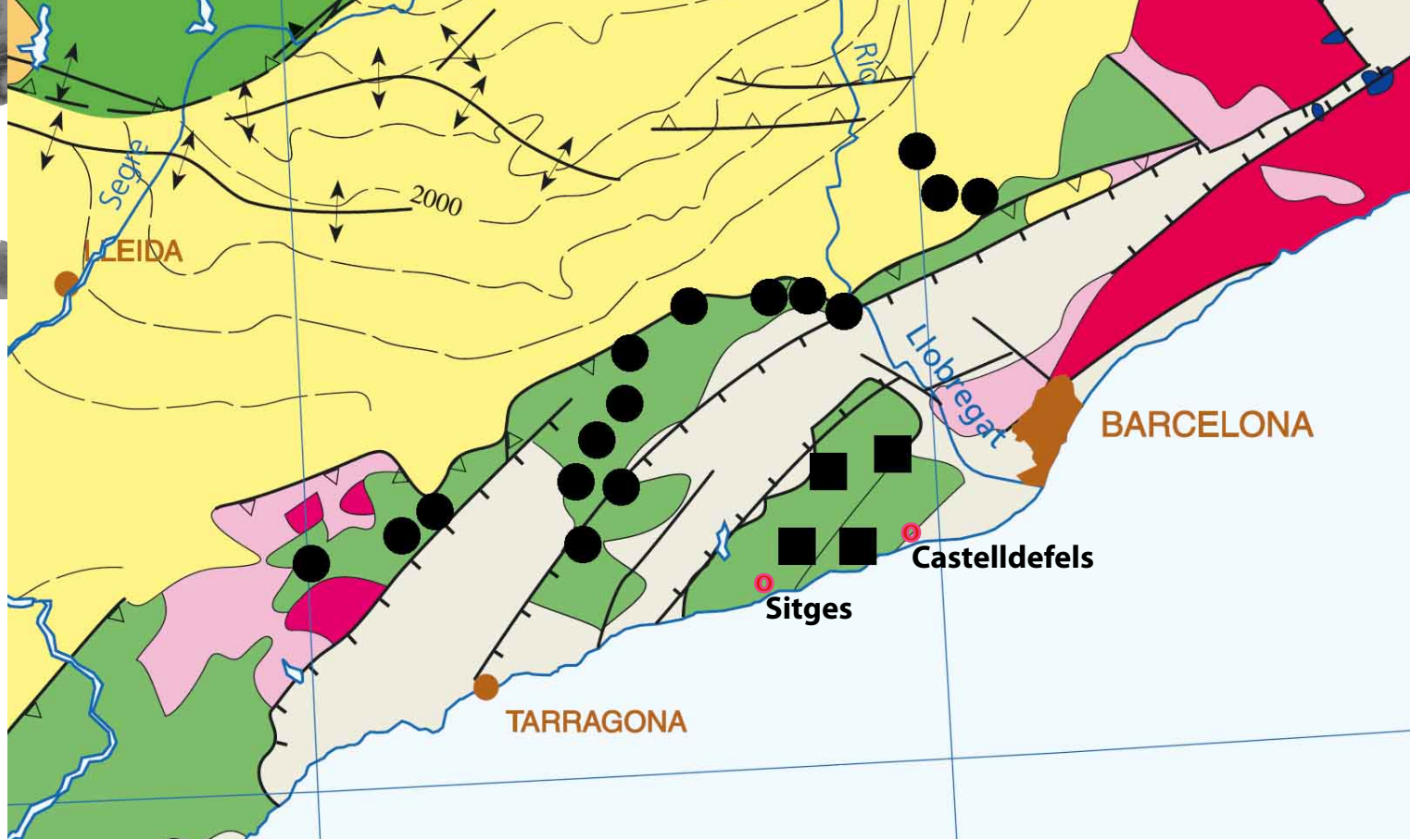
761

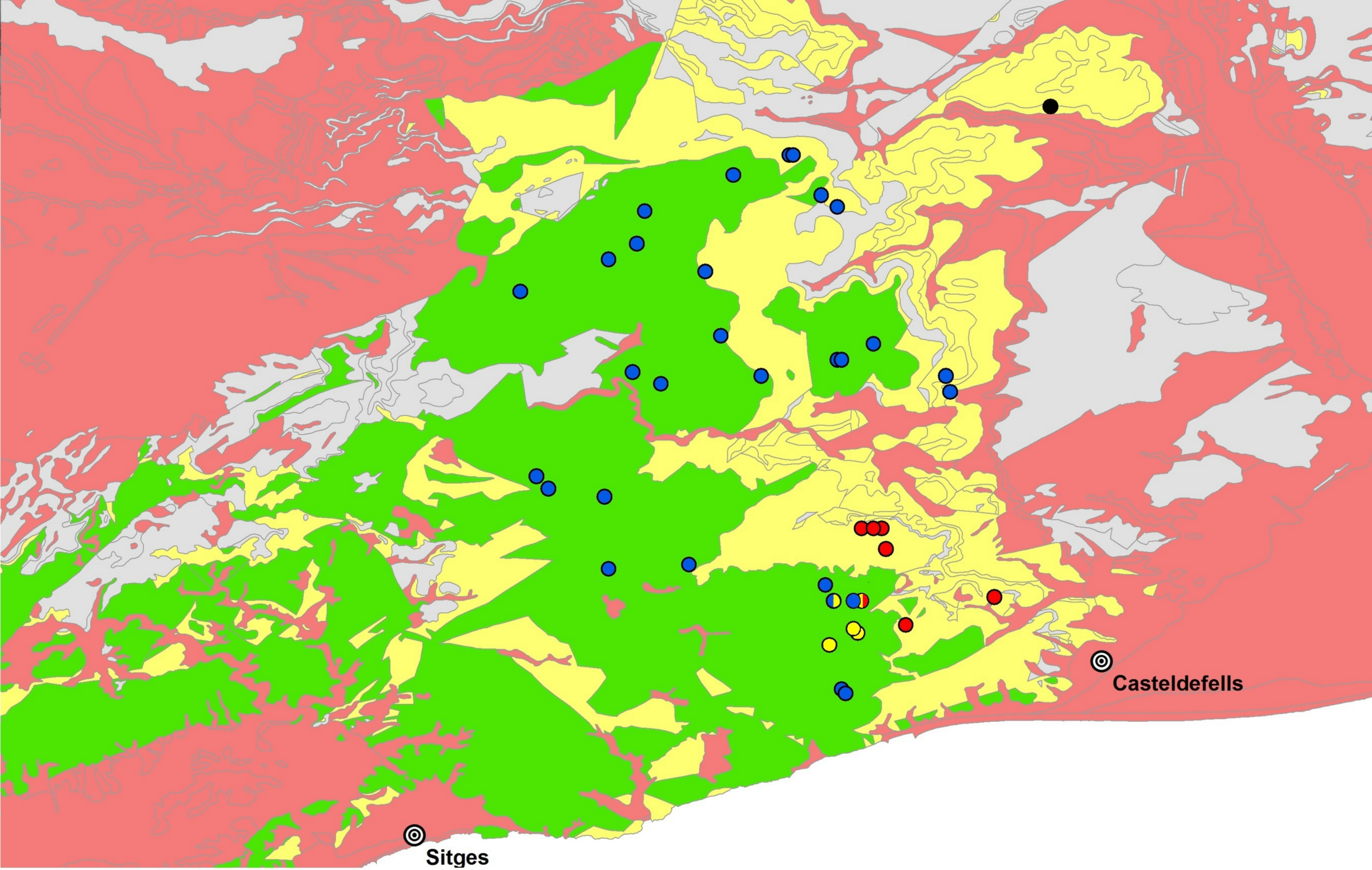
762 **Figure 4** Reconstruction of the ancestral lithology of the substratum in BEAST, using a
763 simplified *coxI-5* matrix and a strict clock with a rate of 0.015 substitutions/site/MY
764 and a constant population size. Numbers in nodes, probabilities of respectively
765 dolostone (red) and limestone (blue) (only when >0). With stars, specimens from caves
766 with fauna of mixed origin (two stars, different main clades; one, different subclades).
767 See Fig. 2 for the location of these caves. Insert: Marginal probability distribution of the
768 reconstructed transition rates from limestone to dolostone (grey) and dolostone to
769 limestone (blue). Habitus photograph by A. Messeger.

770

771

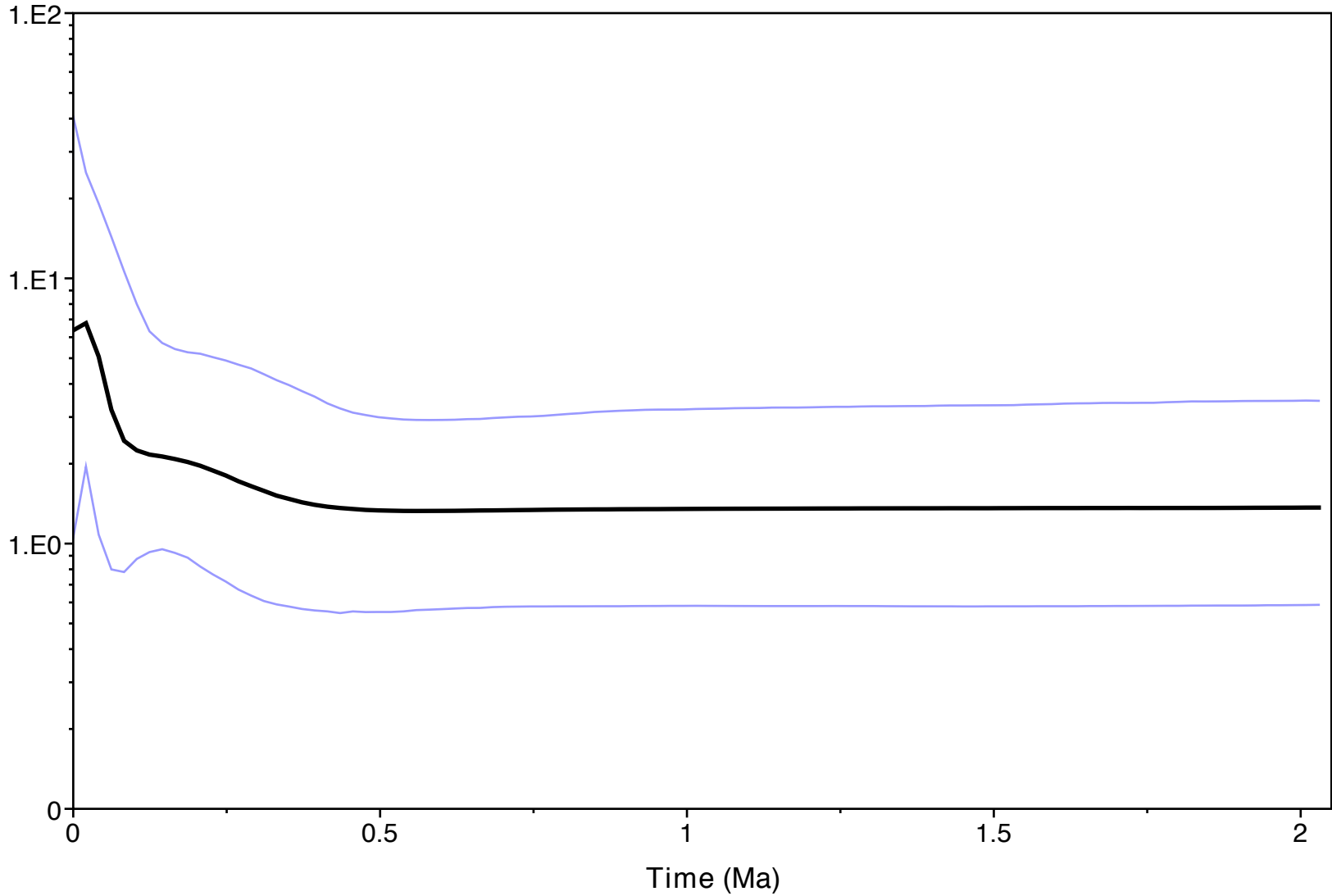
772

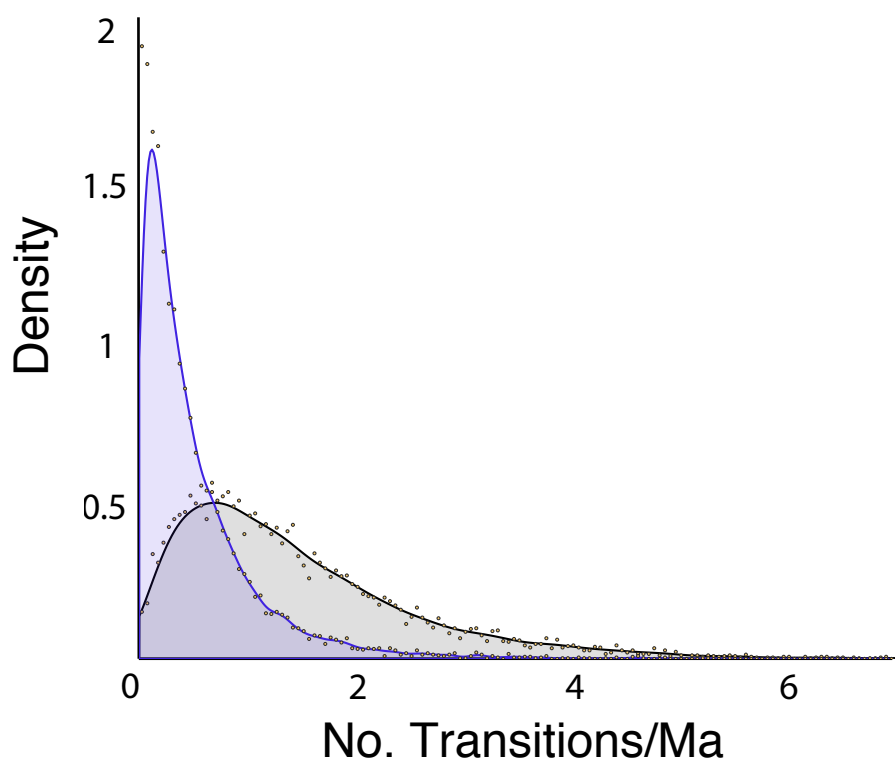




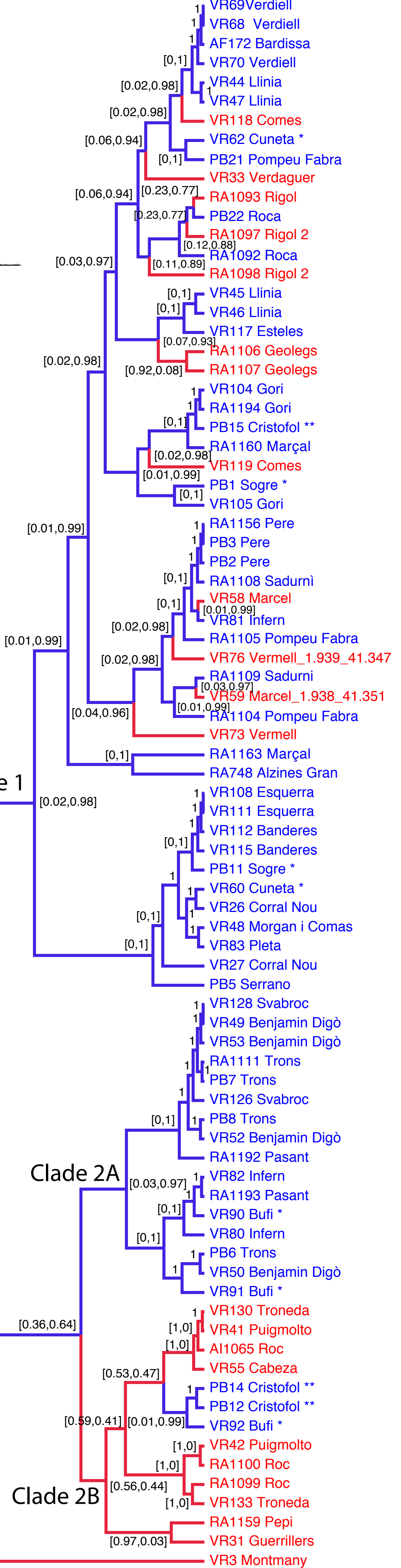
◎
Sitges

◎
Casteldefells





Clade 1



Troglocharinus ferreri

[0.26,0.74]

Clade 2

[0.43,0.57]

Clade 2A

Clade 2B